Molecular Pharmacology Fast Forward. Published on July 12, 2010 as doi: 10.1124/mol.110.065839
This article has not been copyedited and formatted. The final version may differ from this version.

MOL #65839

Title Page

Mechanism-Based Inactivation of Cytochrome P450 3A4 by Lapatinib

Woon Chien Teng, Jing Wen Oh, Lee Sun New, Michelle D. Wahlin, Sidney D. Nelson, Han Kiat Ho, and Eric Chun Yong Chan

Department of Pharmacy, Faculty of Science, National University of Singapore, 18 Science Drive 4, Singapore 117543 (W.C.T., J.W.O, L.S.N, H.K.H., E.C.Y.C.); Department of Medicinal Chemistry, University of Washington, Seattle, WA 98195, USA (M.D.W., S.D.N.); and Institute of Medical Biology, Agency for Science, Technology and Research, 8A Biomedical Grove, Singapore 138648 (H.K.H.)

Molecular Pharmacology Fast Forward. Published on July 12, 2010 as DOI: 10.1124/mol.110.065839
This article has not been copyedited and formatted. The final version may differ from this version.

Running Title Page

Running Title: Mechanism-Based Inactivation of P450 3A4 by Lapatinib

Address correspondence to: Asst Prof. Eric C.Y. Chan, Department of Pharmacy, Faculty of Science, National University of Singapore, 18 Science Drive 4, Singapore 117543, Singapore. Email: phaccye@nus.edu.sg (Asst Prof. H.K. Ho, Email: phahohk@nus.edu.sg)

Number of Text Pages	24
Number of Tables	2
Number of Figures	6
Number of References	35
Number of Words in the Abstract	221
Number of Words in the Introduction	655
Number of Words in the Discussion	1280

ABBREVIATIONS

ACN: Acetonitrile
CO: Carbon monoxide
CYP2C8: Cytochrome P450 2C8 enzyme
CYP3A4: Cytochrome P450 3A4 enzyme
CYP450: Cytochrome P450 enzymes
DDI: Drug-drug interaction
DMSO: Dimethyl sulfoxide
EPI: Enhanced product ion
ESI: Electrospray ionization
FA: Formic acid
GGT: γ-glutamyltransferase
GSH: Reduced L-glutathione
HLM: Human liver microsomes
IDR: Idiosyncratic drug reaction
K_i: Inactivator concentration at half maximum rate of inactivation
k_{inact}: Inactivation rate constant at infinite inactivator concentration
K_{obs}: Observed inactivation rate constant
LC/MS/MS: Liquid chromatography-tandem mass spectrometry
MBI: Mechanism-based inactivator
MIC: Metabolite-intermediate complex
PI: Precursor ion
QTOFMS: Quadrupole, orthogonal acceleration time-of-flight tandem mass spectrometer
RM: Reactive metabolite
R.T.: Retention time

Molecular Pharmacology Fast Forward. Published on July 12, 2010 as DOI: 10.1124/mol.110.065839
This article has not been copyedited and formatted. The final version may differ from this version.

ABSTRACT

Fatalities stemming from hepatotoxicity associated with the clinical use of lapatinib (Tykerb), an oral dual tyrosine kinase inhibitor (ErbB-1 and ErbB-2) used in the treatment of metastatic breast cancer, have been reported. We investigated the inhibition of cytochrome P450 3A4 (CYP3A4) by lapatinib as a possible cause of its idiosyncratic toxicity. Inhibition of CYP3A4 was time-, concentration-, and NADPH-dependent, with k_{inact}=0.0202 min^{-1} and K_i=1.709 μM. The partition ratio was approximately 50.9. Addition of GSH did not affect the rate of inactivation. Testosterone protected CYP3A4 from inactivation by lapatinib. The characteristic Soret peak associated with a metabolite-intermediate complex (MIC) was not observed for lapatinib during spectral difference scanning. However, reduced carbon monoxide (CO)-difference spectroscopy did reveal a 43% loss of the spectrally detectable CYP3A4-CO complex in the presence of lapatinib. Incubation of either lapatinib or its dealkylated metabolite with human liver microsomes (HLM) in the presence of GSH resulted in the formation of a reactive metabolite (RM)-GSH adduct derived from the O-dealkylated metabolite of lapatinib. In addition, co-incubation of lapatinib with ketoconazole inhibited the formation of the RM-GSH adduct. In conclusion, we demonstrated for the first time that lapatinib is a mechanism-based inactivator of CYP3A4 most likely via the formation and further oxidation of its O-dealkylated metabolite to a quinone imine that covalently modifies the CYP3A4 apoprotein and/or heme moiety.

Molecular Pharmacology Fast Forward. Published on July 12, 2010 as DOI: 10.1124/mol.110.065839
This article has not been copyedited and formatted. The final version may differ from this version.

INTRODUCTION

Lapatinib (Fig. 1), the first oral dual tyrosine kinase inhibitor of ErbB-1 and ErbB-2, was approved by the FDA in 2007. As a targeted therapy that inhibits the tyrosine kinase domains on ErbB-1 and ErbB-2, it inhibits downstream cell proliferation and induces apoptosis by the ERK1/2 and PI3K/Akt pathways, respectively (Rusnak et al., 2001; Xia et al., 2002). Lapatinib is usually indicated for co-administration with capecitabine in those patients having the subtype of advanced metastatic breast cancer in which there is ErbB-2 over-expression and resistance to standard therapy such as anthracyclines (e.g. doxorubicin) and taxane (Medina and Goodin, 2008). Both *in vitro* and *in vivo* data further demonstrated lapatinib's effectiveness even in cases resistant to trastuzumab, the first therapeutic monoclonal antibody directed against ErbB-2 (Ryan et al., 2008). The potential of lapatinib's efficacy in metastatic breast cancer has also been demonstrated in various trials (Nelson and Dolder, 2007). Hence, lapatinib presents itself as a promising alternative and orally available drug for the disease.

However, a black boxed warning for lapatinib-related hepatotoxicity was released following post-marketing surveillance and clinical trial reports on elevated liver enzymes and rare cases of liver-related deaths (Gomez et al., 2008). Fatalities stemming from hepatotoxicity associated with its clinical use were also reported recently (European Medicines Agency, 2008). Since the hepatotoxicity of lapatinib has occurred in small numbers of patients and develops several days to months after commencement of therapy, its toxicity appears to be idiosyncratic in nature. To date, the mechanism by which lapatinib causes hepatotoxity is unknown.

Molecular Pharmacology Fast Forward. Published on July 12, 2010 as DOI: 10.1124/mol.110.065839
This article has not been copyedited and formatted. The final version may differ from this version.

Lapatinib is extensively metabolized by cytochrome P450 enzymes (CYP450), in particular CYP3A4/5 and to a lesser extent, CYP2C8 (European Medicines Agency, 2008). Our in-house studies demonstrated that lapatinib is metabolized to form O- and N-dealkylated metabolites, M1 and M2, respectively (Fig. 1). Specifically, the structure of O-dealkylated lapatinib has the potential to generate a reactive quinoneimine similar to the model hepatotoxin acetaminophen (Hinson JA et al., 1981; Dahlin DC et al., 1984). Quinoneimines are electrophilic and have the propensity to react with nucleophilic groups of cellular proteins leading to toxicities. In fact, such bioactivation of drugs to electrophilic reactive species in inducing organ-directed toxicity is one of the most common causes for drug withdrawal (Park et al., 2006). Mechanistically, these electrophilic species may bring about direct covalent modification of hepatic proteins to cause cellular dysfunction, or may form haptens, which in turn trigger an immune response, resulting in hepatotoxicity (Masubuchi and Horie, 2007). Lapatinib has been shown to be a strong inhibitor of CYP3A4 (GlaxoSmithKine, 2007). This information, coupled with its structural predisposition for metabolic activation and reactivity, led us to hypothesize that lapatinib undergoes biotransformation to form reactive electrophilic species that inhibit CYP3A4 irreversibly via mechanism-based inactivation.

CYP3A4 is the most abundant isoform of the CYP450 superfamily in humans. It has broad substrate specificity, and about 60% of xenobiotics are metabolized by CYP3A4. Mechanism-based inactivation of CYP3A4 may lead to accumulation of co-administered drugs in clinical practice, resulting in unforeseen toxicity (Lin et al., 2002). The number of drugs that have been characterized as mechanism-based inactivators (MBIs) has been increasing, due to our greater understanding of its clinical importance.

Molecular Pharmacology Fast Forward. Published on July 12, 2010 as DOI: 10.1124/mol.110.065839
This article has not been copyedited and formatted. The final version may differ from this version.

There are several criteria used in the characterization of MBIs, namely, time-dependency of inactivation; saturable kinetics of inactivation with respect to inhibitor concentration; inactivation in a catalytically competent system; substrate protection of enzyme from inactivation; lack of suppression of inactivation by exogenous nucleophiles; irreversibility of inactivation, and 1:1 binding stoichiometry of inactivator to inactivated enzyme (Rock et al., 2009).

In this study, the nature of CYP3A4 inhibition by lapatinib was investigated based on the criteria in characterizing MBIs. GSH-trapping experiments were also performed to trace the formation of electrophilic reactive metabolites (RMs) of lapatinib that might contribute to any observed covalent modification of CYP3A4. Our results confirmed the generation of an electrophilic RM by lapatinib and established for the first time that lapatinib is a potent MBI of CYP3A4 most likely through oxidation of its O-dealkylated metabolite to a quinone imine.

Molecular Pharmacology Fast Forward. Published on July 12, 2010 as DOI: 10.1124/mol.110.065839
This article has not been copyedited and formatted. The final version may differ from this version.

MATERIALS AND METHODS

Chemicals. HPLC grade methanol and acetonitrile (ACN) were purchased from Tedia Company Inc. (Fairfield, OH, USA). Lapatinib was purchased from LC Laboratories (Woburn, MA, USA). Reduced L-glutathione (GSH), verapamil hydrochloride, ketoconazole, erythromycin, amodiaquine dihydrochloride, quercetin dihydrate, Tergitol NP-40, and Safranin O, were purchased from Sigma Aldrich (St. Louis, MO, USA). Testosterone was purchased from Merck (Darmstadt, Germany). Gemfibrozil glucuronide was purchased from Toronto Research Chemicals Inc (Toronto, Ontario, Canada). Human recombinant P450 3A4 and 2C8 supersomes (rCYP3A4 and rCYP2C8), pooled human liver microsomes (HLM), and NADPH regenerating system were obtained from BD Gentest (Woburn, MA, USA). Water was obtained using a Milli-Q water purification system (Millipore, Bedford, MA, USA). All other reagents used were of analytical grades.

Time-, Concentration-, and NADPH-dependent CYP3A4 Inactivation. Incubations were carried out in 96-well plates. Primary incubations (n=3) consisting of 0.5 mg/ml HLM, 100 mM potassium phosphate buffer (pH 7.4), NADPH B, and lapatinib (1, 2.5, 5, 10, 20, 40, and 50 μM) were prepared. After pre-incubation at 37°C for 6–8 min, the reaction was initiated with the addition of NADPH A. The total volume in each well was 160 μl and the final organic concentrations in the incubation mixture were 0.1% DMSO and 0.9% ACN (v/v). At 0, 3, 8, 15, 22, and 30 min after the addition of NADPH A, 8 μl of the primary incubation were transferred to secondary incubation which contained 200 μM testosterone (probe substrate), NADPH regenerating system, and 100 mM potassium phosphate buffer (pH 7.4). The total volume of secondary reaction

Molecular Pharmacology Fast Forward. Published on July 12, 2010 as DOI: 10.1124/mol.110.065839
This article has not been copyedited and formatted. The final version may differ from this version.

mixture in each well was 160 µl. The secondary incubation mixtures were further incubated for 10 min at 37°C before 50 µl aliquots were removed and quenched with an equal volume of ice-cold ACN and 0.008 µM verapamil (internal standard, IS). In the control incubations, 100 mM potassium phosphate buffer was used in place of NADPH. The same experiment was repeated by replacing lapatinib with erythromycin (1–50 µM) and ketoconazole (0.05–10 µM), a known MBI and competitive inhibitor of CYP3A4, respectively. Samples were centrifuged for 16000 g at 4°C for 15 min and the supernatant was removed for determination of testosterone 6ß-hydroxylation activity by LC/MS/MS. In a separate experiment, rCYP3A4 (20 pmol/ml) replaced HLM. Test compounds (50–500 µM) were incubated for up to 60 min in the primary incubation.

Time-, Concentration-, and NADPH-dependent CYP2C8 Inactivation. Lapatinib (0.1 –10 µM), gemfibrozil glucuronide and quercetin (0.1–50 µM) were prepared in DMSO-acetonitrile (1:1, v/v) while amodiaquine was dissolved in Milli-Q water. The final acetonitrile and DMSO concentrations were less than 1% and 0.04% (v/v), respectively. To investigate the potential of lapatinib as a CYP2C8 MBI, the two-step incubation scheme described in the CYP3A4 assay was used. Gemfibrozil glucuronide is a known MBI of CYP2C8 while quercetin is a known competitive inhibitor. The probe substrate in the secondary incubation was 10 µM amodiaquine.

Partition Ratio. Primary incubations (n=3) comprising of 100 pmol/ml rCYP3A4, NADPH B, lapatinib (1, 1.5, 5, 10, 25, 50 and 75 µM) and 100 mM potassium phosphate buffer were prepared. After pre-incubation at 37°C for 6–8 min, the reaction was initiated by addition of NADPH A and the mixture was incubated at 37°C for another 45 min, allowing it to go to completion. The total volume in each well was 160

Molecular Pharmacology Fast Forward. Published on July 12, 2010 as DOI: 10.1124/mol.110.065839
This article has not been copyedited and formatted. The final version may differ from this version.

µl. 8 µl of the primary incubation was thereafter transferred to the secondary incubation mixture (similar to that prepared for the inactivation studies) and further incubated at 37°C. After 10 min, 50 µl aliquots were removed and quenched as described. In the negative control, the NADPH regenerating system was replaced with 100 mM potassium phosphate buffer in the primary incubation mixture. The samples were centrifuged for 16000 g at 4°C for 15 min and the supernatant was removed for determination of testosterone 6ß-hydroxylation activity by LC/MS/MS.

Effect of Exogenous Nucleophiles. 2 mM GSH was included in the primary incubation mixture (n=3) with 0.5 mg/ml HLM, 50 µM lapatinib, NADPH B and 100 mM potassium phosphate buffer. The reaction was initiated by addition of NADPH A after pre-incubation for 6–8 min at 37°C, to a final volume of 160 µl. 10 µl of aliquots were removed at 0, 4, 8, 15, 22, and 30 min and transferred to secondary incubation mixtures for measurement of residual CYP3A4 activity by LC/MS/MS. Negative controls were prepared by either excluding both GSH and lapatinib, or GSH only in the primary incubation mixture.

Substrate Protection. Excess testosterone (in 1:8 and 1:16 molar ratios of lapatinib:testosterone) was added to the primary incubation mixture (n=3) containing 50 µM lapatinib, 100 pmol/ml rCYP3A4, NADPH B, and 100 mM potassium phosphate buffer. After pre-incubation for 6–8 min at 37°C, NADPH A was added to initiate the reaction. Aliquots were removed at 0, 3, 8, 15, 22, and 30 min and transferred to secondary incubation mixtures similar to that prepared in the time-dependent inhibition assay, and quantification of 6ß-hydroxytestosterone was determined using LC/MS/MS.

Molecular Pharmacology Fast Forward. Published on July 12, 2010 as DOI: 10.1124/mol.110.065839
This article has not been copyedited and formatted. The final version may differ from this version.

Primary reaction mixtures that lacked either testosterone, or both lapatinib and testosterone were prepared as negative controls.

Spectral Difference Scanning. 200 pmol/ml rCYP3A4, NADPH regenerating system and 100 mM potassium phosphate buffer (pH 7.4) were pre-incubated at 37°C for 6–8 min. The reaction was initiated with the addition of 50 μM lapatinib. The sample mixture was immediately scanned from 400 to 500 nm, at 5 min intervals over a 60 min duration using an Infinite M200 Tecan microplate reader (Tecan Group Ltd, Männedorf, Switzerland) which was maintained at 37°C. The spectral differences were obtained by comparing between the sample and reference well (which contained the protein, substrate vehicle and NADPH). The positive control was prepared using 10 μM verapamil.

Reduced CO-difference spectroscopy. Incubations (n=3) were prepared using 50 μM lapatinib, NADPH B, 640 pmol/ml rCYP3A4 in 100 mM potassium phosphate buffer (pH 7.4). After pre-incubation at 37°C for 6–8 min, NADPH A was added to initiate the reaction. The total volume of this mixture was 50 μl and it was further incubated at 37°C. At 30 min, the reaction was terminated by the addition of 450 μl ice-cold quenching buffer which contained 1 mM EDTA, 20% glycerol, 1% Tergitol NP-40, 2 μM Safranin O and 100 mM potassium phosphate buffer (pH 7.4). The resultant mixture was split into two 250 μl tubes (sample and reference tubes). CO was bubbled into one of the tubes (sample tube) and stopped after approximately 60 bubbles had been passed into the mixture. About 1 mg of sodium dithionite was added to both tubes and 220 μl were transferred from each tube into a 96-well plate. The reduced CO-difference spectra for sample and reference wells were acquired by scanning from 400 to 500 nm

Molecular Pharmacology Fast Forward. Published on July 12, 2010 as DOI: 10.1124/mol.110.065839
This article has not been copyedited and formatted. The final version may differ from this version.

using a microplate reader (Guengerich et al., 2009). A negative control was prepared by excluding NADPH from the incubation mixture.

HLM Incubations For Identification of GSH Adducts. Incubation containing 1 mg/ml HLM, NADPH regenerating system, 100 mM potassium phosphate buffer (pH 7.4) and 50 mM GSH were preincubated at 37°C for 6–8 min. The reaction was initiated by the addition of either 5 mM lapatinib or O-dealkylated lapatinib and the total volume of the incubation mixture was 500 µl. The final concentration of each substrate was 50 µM. The synthesis of the O-dealkylated lapatinib metabolite is shown in the supplementary data, Fig. 1. The final concentrations of organic solvents in the incubation were 0.1% DMSO and 0.9% ACN (v/v). At 60 min, 1 ml of ice-cold ACN was added to quench the reaction. The samples were centrifuged at 16000 g for 15 min at 4°C. 1.4 ml of the supernatant was removed and dried under a gentle flow of nitrogen gas (TurboVap LV, Caliper Life Science, Hopkinton, MA, USA). The samples were reconstituted with 100 µl of ACN/water (3/7, v/v), vortex-mixed and centrifuged at 16000 g for 15 min. 90 µL of the supernatant was transferred into the LC/MS vial and 3–5 µL was injected for LC/MS/MS analysis. Negative controls were prepared by the exclusion of either lapatinib, O-dealkylated lapatinib, NADPH or GSH in the incubation mixture. In addition, co-incubation of lapatinib with 0.2 µM ketoconazole was performed separately.

Measurement of Residual CYP3A4 Activity by LC/MS/MS. The LC/MS/MS system consisted of an ACQUITY UPLC system (Waters, Milford, MA, USA) interfaced with a hybrid quadrupole linear ion-trap mass spectrometer equipped with a TurboIonSpray electrospray ionization (ESI) source (QTRAP 3200, Applied Biosystems, Foster City, CA, USA). The UPLC and QTRAP MS systems were both controlled by

Molecular Pharmacology Fast Forward. Published on July 12, 2010 as DOI: 10.1124/mol.110.065839
This article has not been copyedited and formatted. The final version may differ from this version.

Analyst 1.4.2 software (Applied Biosystems). An ACQUITY UPLC BEH C18 1.7 µm 50 × 2.1 mm i.d. column (Waters) was used to achieve chromatographic separation. The column and sample temperatures were 45°C and 4°C, respectively. The mobile phases used were water with 0.1% formic acid (solvent A) and ACN with 0.1% formic acid (solvent B) delivered at a flow rate of 0.5 ml/min. The elution conditions were: linear gradient 22–70% B (0–2.40 min), isocratic 95% B (2.41–2.99 min) and isocratic at 22% B (3.00–3.50 min). Multiple reaction monitoring transitions of *m/z* of 305 to 269 and *m/z* from 455 to 165 were carried out in the ESI positive mode to detect 6ß-hydroxytestosterone and verapamil (IS), respectively. The MS source conditions were: curtain gas (CUR) 20 psi, collision gas (CAD) medium, ionspray voltage (IS) 5500 V, temperature (TEM) 550°C, ion source gas 1 (GS1) 40 psi and ion source gas 2 (GS2) 45 psi. The compound-dependent MS parameters for 6ß-hydroxytestosterone were 6 V, 20 V, and 3 V for entrance potential (EP), collision energy (CE) and collision cell exit potential (CXP), respectively. For verapamil, the EP, CE and CXP were 7 V, 37 V and 2 V, respectively. The declustering potential (DP) and dwell for both 6ß-hydroxytestosterone and verapamil were 52 V and 250 ms, respectively.

Detection of GSH adducts. GSH adducts were analyzed using the same LC/MS/MS system as described above. Chromatographic separation was performed on an ACQUITY UPLC BEH C18 1.7 µm 100 × 2.1 mm i.d. column (Waters). Mobile phases were 0.1% formic acid (FA) in water (solvent A) and 0.1% FA in acetonitrile (solvent B) delivered at 0.45 ml/min. The elution conditions were: linear gradient 5-60% B (0–6.25 min), isocratic 95% B (6.26–7.09 min) and isocratic at 5% B (7.10–8.00 min). The incubated samples were screened for GSH adducts in both electrospray ionization

Molecular Pharmacology Fast Forward. Published on July 12, 2010 as DOI: 10.1124/mol.110.065839
This article has not been copyedited and formatted. The final version may differ from this version.

(ESI) positive and negative modes. Precursor ion (PI) scan experiments at *m/z* 272 were performed in the ESI negative mode. These experiments were used to detect potential GSH adducts in the scan range of *m/z* 400 to 900 in four *m/z* segments. For analyses in ESI positive mode, neutral loss at *m/z* 123 was monitored, while enhanced product ion (EPI) scans were performed for all the potential GSH adducts. The MS source conditions were curtain gas 15 psi, 5500 V or -4500 V, medium, 550°C, 50 psi and 55 psi for CUR, IS, CAD, TEM, GS1 and GS2, respectively. The compound-dependent MS parameters were ±75 V, ±10 V, ±30–40 V, and ±3 V for declustering potential, entrance potential (EP), collision energy (CE) and collision cell exit potential (CXP), respectively.

For the accurate mass profiling of the potential GSH adducts, the incubated samples were analyzed using an ACQUITY UPLC system (Waters) interfaced with a quadrupole, orthogonal acceleration time-of-flight tandem mass spectrometer (QTOFMS) equipped with an ESI source (Q-Tof Premier™, Waters, Manchester, UK). The UPLC/QTOFMS system was controlled by MassLynx 4.1 software (Waters). Chromatographic separations were performed on an ACQUITY UPLC BEH C18 1.7 µm 50 x 2.1 mm i.d. column (Waters). The mobile phases, flow rate and elution conditions were similar to that used for the LC/MS/MS experiments. The QTOFMS system was tuned for optimum sensitivity and resolution in the ESI positive mode using leucine enkephalin (200 pg/uL infused at 5 µL/min). The QTOFMS/MS analysis was operated in the "V" mode and the optimized conditions were as follows: capillary voltage 3200 V, sampling cone 30 V, source temperature 120°C, desolvation temperature 350°C, desolvation gas flow 800 L/h, collision energy 10-20 eV, MCP detector voltage 1900 V, pusher voltage 940 V, pusher voltage offset -1.00 V and puller voltage 725 V. The

Molecular Pharmacology Fast Forward. Published on July 12, 2010 as DOI: 10.1124/mol.110.065839
This article has not been copyedited and formatted. The final version may differ from this version.

precursor mass set at *m/z* of the potential GSH adduct and centroid data were acquired for each sample from 100-900 Da with a 0.2 s scan time and a 0.02 s interscan delay. Prior to analysis, the system was calibrated in the ESI positive mode using a 0.5 M sodium formate solution infused at a flow rate of 5 μL/min. All analyses were acquired using an independent reference spray via the LockSpray™ interface to ensure high mass accuracy and reproducibility; the [M+H]+ ion of leucine enkephalin (2 ng/μL infused at 10 μL/min) was used as the reference lock mass (*m/z* 556.2771). The LockSpray™ was operated at a reference scan frequency, reference cone voltage and collision energy of 10 s, 30 V and 5 eV, respectively.

Data Analysis. All chromatographic peak integration was performed using Analyst 1.4.2. To determine the time-, concentration-, and NADPH-dependent activity in the mechanism-based inactivation assays, the mean of triplicate analyses was used to calculate the natural log of percentage probe substrate activity remaining normalized to 0 min against pre-incubation time. The data were fitted to linear regression and the observed first-order inactivation rate constant, K_{obs}, was determined. Kinetic parameters, K_i and K_{inact}, were determined by a Kitz-Wilson plot (Kitz and Wilson, 1962) to reflect the degree of inactivation of the specific CYP enzyme. These plots were acquired using GraphPad Prism 4.0 (San Diego, CA, USA).

Molecular Pharmacology Fast Forward. Published on July 12, 2010 as DOI: 10.1124/mol.110.065839
This article has not been copyedited and formatted. The final version may differ from this version.

RESULTS

Time-, Concentration-, and NADPH-dependent CYP3A4 Inactivation. Firstly, we investigated the possible involvement of mechanism-based inactivation of CYP3A4 by lapatinib in preincubations with or without NADPH. Testosterone was used as the substrate and the formation of testosterone-6β-hydroxylation was used to measure the enzyme activity. Fig. 2A shows that lapatinib inhibited CYP3A4 in a NADPH-dependent manner. The absence of NADPH in HLM incubations did not show any significant decline in CYP3A4 activity when incubated with lapatinib over the pre-incubation time of 30 min. On the other hand, the presence of NADPH showed a more pronounced concentration- and time-dependent decrease in CYP3A4 activity. This trend was corroborated with lapatinib in rCYP3A4 incubations for up to 60 min (data not shown).

When HLM were pre-incubated with lapatinib in the presence of NADPH for up to 30 min, testosterone-6β-hydroxylation activity declined in a time- and concentration-dependent manner (Fig. 2B). Erythromycin, a known MBI of CYP3A4, and lapatinib demonstrated time-dependent decrease of activity with both HLM and rCYP3A4. On the other hand, the negative control, ketoconazole (a potent competitive CYP3A4 inhibitor), did not show any pre-incubation time-dependent decrease in activity. Similar to erythromycin, lapatinib caused a loss in testosterone hydroxylase activity that followed pseudo-first order kinetics. The kinetic parameters were determined from a Kitz-Wilson plot (Fig 2B, inset). Previously, lapatinib was reported as a mixed-competitive inhibitor with K_i 4 μM (European Medicines Agency, 2008). Under our current experimental conditions, the K_i and k_{inact} values of lapatinib were 1.709 μM and 0.0202 min^{-1}, respectively. The K_i and k_{inact} values of erythromycin were 4.579 μM and 0.0115 min^{-1},

Molecular Pharmacology Fast Forward. Published on July 12, 2010 as DOI: 10.1124/mol.110.065839
This article has not been copyedited and formatted. The final version may differ from this version.

respectively. The determined K_i for ketoconazole was 0.177 μM which is in the range of reported values of 0.004 to 0.180 μM (US Food and Drug Administration, 2006).

Time-, Concentration-, and NADPH-dependent CYP2C8 Inactivation. Amodiaquine-N-desethylation activity (a CYP2C8-selective reaction) decreased to 69.89%, 59.30% and 71.15% of original activity when HLM were incubated for 30 min in the presence of NADPH with 10 μM quercetin, gemfibrozil glucuronide and lapatinib, respectively. The determined K_i for quercetin (competitive inhibitor) and gemfibrozil glucuronide (MBI of CYP2C8) were 0.029 and 0.26 μM, respectively, while the k_{inact} of gemfibrozil glucuronide was 0.015 min^{-1}. Lapatinib and the controls exhibited both time- and concentration-dependent decreases in activity with HLM. However, CYP2C8 inhibition was not increased when HLM were pre-incubated with quercetin and lapatinib in the presence of NADPH. Conversely, a significant decrease in CYP2C8 activity was observed when gemfibrozil glucuronide was pre-incubated with HLM plus a NADPH-regenerating system. Hence, our observations suggested that lapatinib is not a MBI of CYP2C8.

Partition Ratio. A titration method (Silverman, 1995) was used to determine the partition ratio, which is the number of inactivator molecules metabolized per molecule of enzyme inactivated. Metabolism of lapatinib using rCYP3A4 was performed to completion and 6ß-hydroxytestosterone was used to measure residual CYP3A4 activity. Lapatinib was incubated with rCYP3A4 in the presence of NADPH for 45 min until the reaction was completed. Fig. 3A shows the plot of residual CYP3A4 activity versus molar ratios of lapatinib to CYP3A4. Extrapolating the intercept of the linear regression

Molecular Pharmacology Fast Forward. Published on July 12, 2010 as DOI: 10.1124/mol.110.065839
This article has not been copyedited and formatted. The final version may differ from this version.

line at lower ratios and the straight line for the higher ratios to the x-axis gave a turnover number of 51.9. Subtracting one from this value yielded a partition ratio of 50.9.

Effect of Exogenous Nucleophiles and Alternate Substrate on Inactivation. Addition of GSH (exogenous nucleophile) did not affect the rate of enzyme inactivation. As shown in Fig. 3B, CYP3A4 was inactivated to a similar extent as compared to that during incubation with lapatinib alone. Co-incubation with 8- and 16-fold excess of testosterone, an alternate substrate of CYP3A4, protected the enzyme from inactivation by lapatinib, as seen in the diminished rate of inactivation with time (Fig. 3C).

Spectral Difference Scanning. MIC-forming compounds tend to show a characteristic peak in the Soret region (448–458 nm) (Polasek and Miners, 2008). When spectral differences were obtained by scanning from 400 to 500 nm for 60 min, lapatinib did not show any observable peak in the Soret region when incubated with CYP3A4 (Fig. 3D) while verapamil (a known MIC of CYP3A4) produced a clear peak at 448–458 nm (supplementary data, Fig. 2).

Reduced CO-difference spectroscopy. Ferrous (reduced) cytochrome P450 forms a complex with CO to give a spectrally detectable peak at 450 nm. Using the formula for calculating CYP450 concentration ([ΔA450–ΔA490]/0.091=nmol of P450 per ml) (Guengerich et al., 2009), the extent of reduction in the 450 nm peak was derived. When 50 μM lapatinib was incubated with CYP3A4 for 30 min, there was a 43 ± 7.8% decrease in the peak at 450 nm (n=3) as compared to the control incubation in the absence of NADPH.

Identification of GSH adducts. To determine if generation of RMs was the cause for lapatinib-induced toxicity, GSH-trapping was performed on lapatinib-HLM

Molecular Pharmacology Fast Forward. Published on July 12, 2010 as DOI: 10.1124/mol.110.065839
This article has not been copyedited and formatted. The final version may differ from this version.

incubations. Pre-screening of GSH-adducts with metabolites of lapatinib were conducted over five separate *m/z* ranges from *m/z* 400 to 900 to ensure optimal MS sensitivity. One peak with *m/z* 778 (LAPA-G1; R.T. 2.03 min) suggestive of a GSH adduct was observed in the precursor scan at *m/z* 272 in the ESI negative mode and was not observed in any of the negative controls (Fig. 4A). Co-incubation with ketoconazole resulted in reduction of the peak (Fig. 4B). The GSH-trapping assay was repeated by incubating O-dealkylated lapatinib in HLM and both LAPA-G1 and LAPA-G2 were also observed in the LC/MS/MS analysis (Fig. 4C).

The EPI scans of LAPA-G1 (Fig. 5A) generated a spectrum characteristic of collision-induced dissociation fragmentation of GSH where there was a neutral mass loss of 129 corresponding to loss of the pyroglutamic acid moiety. Neutral loss scan at *m/z* 123 was further performed to profile any additional GSH adducts that shared a similar fragmentation pattern to LAPA and a peak at 1.83 min (*m/z* 649) was detected (Fig. 4 and 5B). To further confirm the identity of the potential GSH adduct, accurate mass measurements were performed using QTOFMS. The program MassLynx was used to determine the potential calculated masses, mass accuracy (mDa and ppm), i-FIT (Norm) (the likelihood that the isotopic pattern of the elemental composition matches a cluster of peaks in the spectrum) values and elemental compositions associated with the measured mass of the GSH adducts and their fragments were generated and summarized in Table 1.

Molecular Pharmacology Fast Forward. Published on July 12, 2010 as DOI: 10.1124/mol.110.065839
This article has not been copyedited and formatted. The final version may differ from this version.

DISCUSSION

Mechanism-based inactivation of P450 enzymes is preceded by formation of a reactive intermediate, and therefore requires NADPH and exhibits both time- and concentration-dependence (Ito et al., 1998). Lapatinib was found to inhibit CYP3A4 in accordance with these criteria with reproducible K_i and k_{inact} values, using a catalytically competent system. We attested the reliability of our data by measuring the K_i and k_{inact} values of the classic CYP3A4 MBI, erythromycin, and found values consistent with those in the published literature (Table 2). Notably, the k_{inact}/K_i ratio for lapatinib was lower than that observed for troleandomycin, but higher than clinically relevant MBIs such as erythromycin, dihydralazine and clarithromycin. Erythromycin can cause Torsades de pointes when co-administered with terfenadine, cisapride or astemizole, and rhabdomyolysis with simvastastin (Spinler et al., 1995) through DDIs. Likewise, dihydralazine had been reported to induce immunoallergic hepatitis (Masubuchi and Horie, 1999). Therefore, it is reasonable to postulate that lapatinib, being an even more potent MBI, may be capable of inducing hepatotoxicity through DDI and/or immune-mediated toxicity (Uetrecht, 2007). However, additional clinical data and development of an animal model will be required to determine the exact mechanism of lapatinib-mediated hepatotoxicity.

A MBI's efficiency is estimated by its partition ratio, which is the number of times each CYP450 turns over the drug before a reactive intermediate inactivates the enzyme. The measured partition ratio for lapatinib was 50.9, a relatively high value compared to those reported for numerous CYP3A4 MBIs (Ghanbari et al., 2006). Co-incubation with GSH did not affect the rate of CYP3A4 inactivation by lapatinib, which

Molecular Pharmacology Fast Forward. Published on July 12, 2010 as DOI: 10.1124/mol.110.065839
This article has not been copyedited and formatted. The final version may differ from this version.

suggests that the RM was formed and inactivated by the enzyme prior to its release from the active site. Co-incubation with an alternate substrate, testosterone, protected CYP3A4 from inactivation, further confirming that inactivation by lapatinib occurred at the enzyme's active site. These novel findings collectively substantiated mechanism-based inactivation of CYP3A4 by lapatinib.

At least three mechanisms of inactivation of CYP450 by MBIs have been proposed, namely, alkylation of the P450 heme moiety, modification of P450 apoprotein, and formation of a coordinate covalent bond with the heme iron that results in a metabolite-intermediate complex (MIC) (Polasek and Miners, 2007). Spectral analyses were performed to elucidate the mechanistic details of CYP3A4 inactivation by lapatinib. The absence of a Soret peak ruled out the possibility of pseudo-irreversible MIC formation by lapatinib, which suggests that CYP3A4 was irreversibly inactivated by a lapatinib metabolite, most likely via covalent modification of the enzyme. This possibility was supported by reduced CO-difference spectroscopy which showed a 43% loss of spectrally detectable CYP3A4-CO complex at 450 nm in the presence of lapatinib accompanied by an increase in absorption at 420 nm. While reduction in absorption at 450 nm could be linked to either heme adduction or heme destruction, covalent adduction of a RM to apo-protein in close proximity to the heme moiety could compromise the integrity of the CYP3A4 active site. This could, thereby, interfere with CO-heme binding and lead to an increase in absorption at 420 nm (Omura T and Sato R, 1964). Covalent adduction to apo-protein has been demonstrated for MBIs such as bergamottin (He et al., 1998) and mifepristone (He et al., 1999), while the MBI formed from 17α-ethynylestradiol forms adducts to both heme and apo-protein (Lin et al., 2002). Although

Molecular Pharmacology Fast Forward. Published on July 12, 2010 as DOI: 10.1124/mol.110.065839
This article has not been copyedited and formatted. The final version may differ from this version.

further work is required to determine how lapatinib inhibits CYP3A4 at the molecular level, we hypothesize that the quinoneimine of the O-dealkylated metabolite of lapatinib binds to the apoprotein of CYP3A4, since it is a relatively soft electrophile that would react with soft nucleophiles on proteins.

The *para*-aminophenol group of the O-dealkylated metabolite of lapatinib (M1, Fig. 1) provided an initial structural alert to its potential toxicity mechanism since it could be oxidized to the reactive quinoneimine species, based on parallels of studies with N-acetyl-*p*-benzo-quinoneimine generated from the cytochrome P450 oxidation of acetaminophen (Dahlin et al., 1984; Albano et al., 1985). Moreover, it was confirmed that lapatinib did not inhibit CYP2C8 as a MBI, although it is a competitive inhibitor for this enzyme, which suggests that lapatinib may be metabolized differently or to a different extent by CYP3A4 as compared to CYP2C8. A RM-GSH adduct, LAPA-G1, was identified in the present study, (Fig. 4). The accurate mass-to-charge (*m/z*) ratios of the parent and product ions of LAPA-G1 fell within 5 ppm (Table 1A). Coupled to the strong i-FIT values (< 5 units) that indicated good fit with the isotopic pattern of each ion, our confidence in the assignment of elemental compositions of the parent and product ions was significantly enhanced. The RM was a quinoneimine generated from the oxidation of the *para*-aminophenol group of the O-dealkylated metabolite (LAPA-G1; *m/z* 778; Fig. 5A). This was further confirmed by the detection of LAPA-G1 in the incubated sample of O-dealkylated lapatinib with HLM and GSH (Fig 4C). The proposed bioactivation pathway of lapatinib is summarized in Fig. 6. This bioactivation parallels that of other structurally similar tyrosine kinase inhibitors such as dasatinib (Li et al., 2009) and gefitinib (Li et al., 2009) which have been shown to form similar reactive

Molecular Pharmacology Fast Forward. Published on July 12, 2010 as DOI: 10.1124/mol.110.065839
This article has not been copyedited and formatted. The final version may differ from this version.

quinone metabolites and cause idiosyncratic heptatotoxicity. Addition of ketoconazole, a reversible competitive CYP3A4 inhibitor, reduced formation of the RM-GSH adduct *in vitro* (Fig. 4B), confirming that the RM was generated from oxidative metabolism by CYP3A4.

Interestingly, another adduct, LAPA-G2 (*m/z* 649), was observed and confirmed to be metabolically-derived (Fig. 4). Its fragmentation pattern lacked the characteristic neutral loss of 129 associated with a typical RM-GSH adduct (Fig. 5B). It was also noted that the mass difference between LAPA-G1 and G2 was 129, corresponding to the loss of the pyroglutamic acid moiety of GSH. Furthermore, LAPA-G2 demonstrated fragmentation losses of 123 and a fragment ion at *m/z* 382, of all which are characteristic of the fragmentation pattern of lapatinib. The accurate mass-to-charge (*m/z*) ratios of the parent and product ions of LAPA-G2 are within 5 ppm (Table 1B) and low i-FIT values (< 3 units). These collectively suggested that LAPA-G2 was a cysteinylglycine conjugate, the secondary metabolite of LAPA-G1 derived from the mercapturate pathway as catalyzed by γ-glutamyltransferase (GGT), a human liver microsomal enzyme (Fig. 6). In GSH conjugation of xenobiotics, the mercapturate pathway is a common detoxification route (Stevens, 1989).

Our results raise the possibility that lapatinib-related hepatotoxicity may be an idiosyncratic drug reaction (IDR) which occurs at continuous high dosing. This is in agreement with reports of C_{max} and AUC increases that are more than dose-proportional with continuous dosing (European Medicines Agency, 2008). While IDRs are said to be dose-independent, an apparent dose-response relationship amongst those at risk may arise from increased cellular protein-RM binding, as demonstrated by the correlation between

Molecular Pharmacology Fast Forward. Published on July 12, 2010 as DOI: 10.1124/mol.110.065839
This article has not been copyedited and formatted. The final version may differ from this version.

the risks of IDRs for halogenated anaesthetics and the amount of trifluoroacetyl halide RM formed (Njoku et al., 1997). It was observed that drugs administered at less than 10 mg/day are generally rarely associated with IDRs (Uetrecht, 1999) while drugs dosed more than 1 g/day (e.g. felbamate) are more likely to cause IDRs (Uetrecht, 2007). Hence, the 1.25 g/day dosing for lapatinib (European Medicines Agency, 2008) could reasonably exceed the threshold level for toxicity in a susceptible subpopulation. Therefore, any involvement of immuno-hepatotoxicity with lapatinib could not be excluded. In fact, the high therapeutic dose of lapatinib, coupled to its efficiency as a CYP3A4 MBI, could presumably trigger protein modification and immune response, such as with tienilic acid, which caused rare idiosyncratic hepatotoxicity upon mechanism-based inactivation of CYP2C9, resulting in antibodies formation against CYP2C9 (Masubuchi and Horie, 2007). Nevertheless, although IDRs appear to be RM-driven and immune-mediated, host genetic and environmental influences can also be contributory (Uetrecht, 2007). Hence, the clinical characteristics of lapatinib-related hepatotoxicity are crucial in understanding the toxicity mechanism.

In conclusion, we demonstrated for the first time that lapatinib is a CYP3A4 MBI via covalent modification of its apoprotein and/or heme moiety, and elucidated the structure of the RM possibly involved in the irreversible inactivation of the enzyme. Future preclinical and clinical studies are needed to further confirm the mechanism of toxicity of lapatinib.

Molecular Pharmacology Fast Forward. Published on July 12, 2010 as DOI: 10.1124/mol.110.065839
This article has not been copyedited and formatted. The final version may differ from this version.

REFERENCES

Albano E, Rundgren M, Harvison PJ, Nelson SD and Moldéus P (1985) Mechanisms of N-acetyl-p-benzoquinone imine cytotoxicity. *Mol Pharmacol* **28:**306-311.

Dhalin DC, Miwa GT, Lu AYH and Nelson SD (1984) N-acetyl-p-benzoquinone imine - a cytochrome-P-450-mediated oxidation-product of acetaminophen. *P Natl Acad Sci USA* **81**:1327-1331.

European Medicines Agency (25 Nov 2008) Assessment report for tyverb. http://www.emea.europa.eu/humandocs/PDFs/EPAR/tyverb/H-795-en6.pdf (accessed 18 Jan 2009).

Ghanbari F, Rowland-Yeo K, Bloomer JC, Clarke SE, Lennard MS, Tucker GT and Rostami-Hodjegan A (2006) A critical evaluation of the experimental design of studies of mechanism based enzyme inhibition, with implications for in vitro-in vivo extrapolation. *Curr Drug Metab* **7:**315-334.

GlaxoSmithKine (2007) Tykerb® Product Information.

Gomez HL, Doval DC, Chavez MA, Ang PCS, Aziz Z, Nag S, Ng C, Franco SX, Chow LWC, Arbushites MC, Casey MA, Berger MS, Stein SH and Sledge GW (2008) Efficacy and safety of lapatinib as first-line therapy for ErbB2-amplified locally advanced or metastatic breast cancer. *J Clin Oncol* **26:**2999-3005.

Guengerich FP, Martin MV, Sohl CD and Cheng Q (2009) Measurement of cytochrome P450 and NADPH-cytochrome P450 reductase. *Nat Protoc* **4:**1245-1251.

He K, Iyer KR, Hayes RN, Sinz MW, Woolf TF and Hollenberg PF (1998) Inactivation of cytochrome P450 3A4 by bergamottin, a component of grapefruit juice. *Chem Res Toxicol* **11:**252-259.

He K, Woolf TF and Hollenberg PF (1999) Mechanism-based inactivation of cytochrome P-450-3A4 by mifepristone (RU486). *J Pharmacol Exp Ther* **288:**791-797.

Hinson JA, Pohl LR and Monks TJ and Gillette JR. (1981) Acetaminophen-induced hepatotoxicity. *Life Sci* **29:**107-116.

Ito K, Iwatsubo T, Kanamitsu S, Ueda K, Suzuki H and Sugiyama Y (1998) Prediction of pharmacokinetic alterations caused by drug-drug interactions: metabolic interaction in the liver. *Pharmacol Rev* **50:**387-412.

Kitz R and Wilson IB (1962) Esters of methanesulfonic acid as irreversible inhibitors of acetylcholinesterase. *J Biol Chem* **237:**3245-3249.

Li X, He Y, Ruiz CH, Koenig M and Cameron MD (2009) Characterization of dasatinib

and its structural analogs as CYP3A4 mechanism-based inactivators and the proposed bioactivation pathways. *Drug Metab Dispos* **37:**1242-1250.

Li X, Kamenecka TM and Cameron MD (2009) Bioactivation of the epidermal growth factor receptor inhibitor gefitinib: implications for pulmonary and hepatic toxicities. *Chem Res Toxicol* **22:**1736-1742.

Lin HL, Kent UM and Hollenberg PF (2002) Mechanism-based inactivation of cytochrome P450 3A4 by 17 alpha-ethynylestradiol: evidence for heme destruction and covalent binding to protein. *J Pharmacol Exp Ther* **301:**160-167.

Masubuchi Y and Horie T (2007) Toxicological significance of mechanism-based inactivation of cytochrome p450 enzymes by drugs. *Crit Rev Toxicol* **37:**389-412.

Masubuchi Y and Horie T (1999) Mechanism-based inactivation of cytochrome P450s 1A2 and 3A4 by dihydralazine in human liver microsomes. *Chem Res Toxicol* **12:**1028-1032.

Medina PJ and Goodin S (2008) Lapatinib: a dual inhibitor of human epidermal growth factor receptor tyrosine kinases. *Clin Ther* **30:**1426-1447.

Nelson MH and Dolder CR (2007) A review of lapatinib ditosylate in the treatment of

refractory or advanced breast cancer. *Therapeutics and clinical risk management* **3:**665-673.

Njoku D, Laster MJ, Gong DH, Eger EI, Reed GF and Martin JL (1997) Biotransformation of halothane, enflurane, isoflurane, and desflurane to trifluoroacetylated liver proteins: association between protein acylation and hepatic injury. *Anesth Analg* **84:**173-178.

Omura T and Sato R (1964) Isolation of cytochromes P-450 and P-420. *Methods Enzymol* **239:**1018.

Park KB, Dalton-Brown E, Hirst C and Williams DP (2006) Selection of new chemical entities with decreased potential for adverse drug reactions. *Eur J Pharmacol* **549:**1-8.

Polasek TM and Miners JO (2006) Quantitative prediction of macrolide drug-drug interaction potential from in vitro studies using testosterone as the human cytochrome P4503A substrate. *Eur J Clin Pharmacol* **62:**203-208.

Polasek TM and Miners JO (2007) In vitro approaches to investigate mechanism-based inactivation of CYP enzymes. *Expert Opin Drug Metab Toxicol* **3:**321-329.

Polasek TM and Miners JO (2008) Time-dependent inhibition of human drug

metabolizing cytochromes P450 by tricyclic antidepressants. *Br J Clin Pharmacol* **65:**87-97.

Rock D, Schrag M and Wienkers LC (2009) Experimental Characterization of Cytochrome P450 Mechanism Based Inhibition, in *Handbook of Drug Metabolism* (Pearson PG WL, eds) pp 541-569, Informa HealthCare, UK.

Rusnak DW, Affleck K, Cockerill SG, Stubberfield C, Harris R, Page M, Smith KJ, Guntrip SB, Carter MC, Shaw RJ, Jowett A, Stables J, Topley P, Wood ER, Brignola PS, Kadwell SH, Reep BR, Mullin RJ, Alligood KJ, Keith BR, Crosby RM, Murray DM, Knight WB, Gilmer TM and Lackey K (2001) The characterization of novel, dual ErbB-2/EGFR, tyrosine kinase inhibitors: potential therapy for cancer. *Cancer Res* **61:**7196-7203.

Ryan Q, Ibrahim A, Cohen MH, Johnson J, Ko CW, Sridhara R, Justice R and Pazdur R (2008) FDA drug approval summary: lapatinib in combination with capecitabine for previously treated metastatic breast cancer that overexpresses HER-2. *Oncologist* **13:**1114-1119.

Silverman RB (1995) Mechanism-based enzyme inactivators. *Methods Enzymol* **249:**240-283.

Spinler SA, Cheng JW, Kindwall KE and Charland SL (1995) Possible inhibition of hepatic metabolism of quinidine by erythromycin. *Clin Pharmacol Ther* **57:**89-94.

Stevens JL (1989) The Mercapturic Acid Pathway - Biosynthesis, Intermediary Metabolism, and Physiological Disposition, in *Glutathione chemical, biochemical, and medical aspects* (Dolphin D; Avramović OandPoulson R, eds) pp 930, John Wiley and Sons, New York.

US Food and Drug Administration (1 May 2006) Drug Development and Drug Interactions: Table of Substrates, Inhibitors and Inducers. http://www.fda.gov/Drugs/DevelopmentApprovalProcess/DevelopmentResources/DrugInteractionsLabeling/ucm081177.htm (accessed 25 February 2010).

Uetrecht JP (1999) New concepts in immunology relevant to idiosyncratic drug reactions: the "danger hypothesis" and innate immune system. *Chem Res Toxicol* **12:**387-395.

Uetrecht JP (2007) Idiosyncratic drug reactions: current understanding. *Annu Rev Pharmacol Toxicol* **47:**513-539.

Xia W, Mullin RJ, Keith BR, Liu LH, Ma H, Rusnak DW, Owens G, Alligood KJ and Spector NL (2002) Anti-tumor activity of GW572016: a dual tyrosine kinase inhibitor

Molecular Pharmacology Fast Forward. Published on July 12, 2010 as DOI: 10.1124/mol.110.065839
This article has not been copyedited and formatted. The final version may differ from this version.

blocks EGF activation of EGFR/erbB2 and downstream Erk1/2 and AKT pathways. *Oncogene* **21:**6255-6263.

Molecular Pharmacology Fast Forward. Published on July 12, 2010 as DOI: 10.1124/mol.110.065839
This article has not been copyedited and formatted. The final version may differ from this version.

Footnotes:

This work was supported by the National University of Singapore (NUS) grants [R-148-000-100-112, R-279-000-249-646 and R-148-000-117-133], NUS Department of Pharmacy Final Year Project grant [R-148-000-003-001] and Biomedical Research Council, A*STAR.

Molecular Pharmacology Fast Forward. Published on July 12, 2010 as DOI: 10.1124/mol.110.065839
This article has not been copyedited and formatted. The final version may differ from this version.

LEGENDS FOR FIGURES

Fig. 1 Chemical structures of lapatinib and its two major metabolites, M1 (O-dealkylated lapatinib) and M2 (N-dealkylated lapatinib). The formation of M1 and M2 is mediated by both CYP3A4 (major) and CYP2C8 (minor).

Fig. 2 (A) NADPH-dependent inactivation of CYP3A4 by lapatinib. 50 μM lapatinib was incubated in the presence and absence of NADPH. (B) Time- and concentration-dependent inactivation of CYP3A4 by lapatinib. The concentrations of lapatinib used were 0, 2.5, 5, 10, 20, and 50 μM. The inset shows the Kitz-Wilson plot. Values of k_{inact} and K_i are 0.0202 min^{-1} and 1.709 μM, respectively. For both plots, each point represents the mean from three replicates with less than 10% S.D.

Fig. 3 (A) Determination of the partition ratio for inactivation of CYP3A4 by lapatinib; the estimated partition ratio of 50.9 was determined by extrapolating the intercept of the linear regression line at lower ratios and the straight line for the higher ratios to the x-axis. (B) Effect of GSH on residual CYP3A4 activity. Pooled HLM were incubated with either 2 mM GSH and 50 μM lapatinib (□), 50 μM lapatinib alone (■), or neither lapatinib nor GSH (▼), in the presence of NADPH. (C) Substrate protection of CYP3A4 with testosterone. rCYP3A4 was incubated with 50 μM lapatinib (■), 1:8 lapatinib:testosterone (○), 1:16 lapatinib:testosterone (▲), and neither lapatinib nor testosterone (×), in the presence of NADPH. (D) Absorbance difference as a function of wavelength. 50 μM lapatinib was incubated with rCYP3A4 in the presence of NADPH. Reference wells contained an equivalent volume of solvent in place of substrate. Spectral differences between sample and reference wells were acquired by scanning from 400 to

500 nm every 5 min for 60 min. For plots A-C, each point represents the mean from three replicates with less than 10% S.D.

Fig. 4 MRM chromatograms of HLM incubations with GSH with (A) 50 μM lapatinib, (B) 50 μM lapatinib and 0.2 μM ketoconazole and (C) 50 μM O-dealkylated lapatinib. The adducts are labelled as LAPA-G1 and LAPA-G2.

Fig. 5 Enhanced product ion scans of (A) LAPA-G1 (*m/z* 778) and (B) LAPA-G2 (*m/z* 649).

Fig. 6 Proposed bioactivation pathway of lapatinib by CYP3A4.

Molecular Pharmacology Fast Forward. Published on July 12, 2010 as DOI: 10.1124/mol.110.065839
This article has not been copyedited and formatted. The final version may differ from this version.

Table 1. Summarized results of the QTOFMS analyses of the parent and product ions of LAPA-G1 (*m/z* 778) and LAPA-G2 (*m/z* 649) using a mass tolerance of 10 ppm.

Chemical formula	**Theoretical *m/z***	**Experimental *m/z***	**mDa**	**ppm**	**i-FIT (Norm)**
$C_{32}H_{37}ClN_7O_{10}S_2$	778.1732	778.1725	-0.7	-0.9	2.3
$C_{29}H_{28}ClN_6O_8S$	655.1378	655.1353	-2.5	-3.8	3.2
$C_{27}H_{30}ClN_6O_7S_2$	649.1306	649.1308	0.2	0.3	0.9
$C_{24}H_{21}ClN_5O_5S$	526.0952	526.0944	-0.8	-1.5	4.2
$C_{19}H_{13}ClN_3O_2S$	382.0417	382.0410	-0.7	-1.8	2.3

Chemical formula	**Theoretical *m/z***	**Experimental *m/z***	**mDa**	**ppm**	**i-FIT (Norm)**
$C_{27}H_{30}ClN_6O_7S_2$	649.1306	649.1302	-0.4	-0.6	1.9
$C_{24}H_{21}ClN_5O_5S$	526.0952	526.0939	-1.3	-2.5	2.5
$C_{19}H_{13}ClN_3O_2S$	382.0417	382.0414	-0.3	-0.8	2.1

Molecular Pharmacology Fast Forward. Published on July 12, 2010 as DOI: 10.1124/mol.110.065839
This article has not been copyedited and formatted. The final version may differ from this version.

Table 2: Comparison of enzyme inactivation kinetic constants for the various mechanism-based inactivators and competitive inhibitor of CYP3A4 using testosterone-6β-hydroxylation as an indication of CYP3A4 residual activity.

Compound	Enzyme source	K_i (μM)	k_{inact} (min^{-1})	k_{inact}/K_i ($min^{-1}.mM^{-1}$)	Reference
Ketoconazole	HLM	0.0037 – 0.18[1]	-	-	FDA, 2006
Ketoconazole	HLM	0.177[1]	-	-	From in-house data
Erythromycin	HLM	12.8	0.037	2.891[2]	(Polasek and Miners, 2006)
Erythromycin	rCYP3A4	0.92	0.058	63.043[2]	
Erythromycin	HLM	4.579	0.0115	2.511	From in-house data
Lapatinib	HLM	2.679	0.0212	7.913	From in-house data
Dihydralazine	HLM	35.0	0.0495	1.414[2]	Masubuchi and Horie, 1999
Clarithromycin	HLM	29.5	0.050	1.695[2]	Polasek and Miners, 2006
Clarithromycin	rCYP3A4	2.25	0.040	17.778[2]	
Mifepristone	rCYP3A4	4.7	0.089	18.936[2]	He et al., 1999
Troleandomycin	HLM	0.14	0.027	192.857[2]	Polasek and Miners, 2006
Troleandomycin	rCYP3A4	0.08	0.054	675.000[2]	

[1] *Ketoconazole is a competitive inhibitor of CYP3A4 but not a mechanism-based inactivator.*
[2] *Calculated from reported K_i and k_{inact}.*

Molecular Pharmacology Fast Forward. Published on July 12, 2010 as DOI: 10.1124/mol.110.065839
This article has not been copyedited and formatted. The final version may differ from this version.

Figure 1

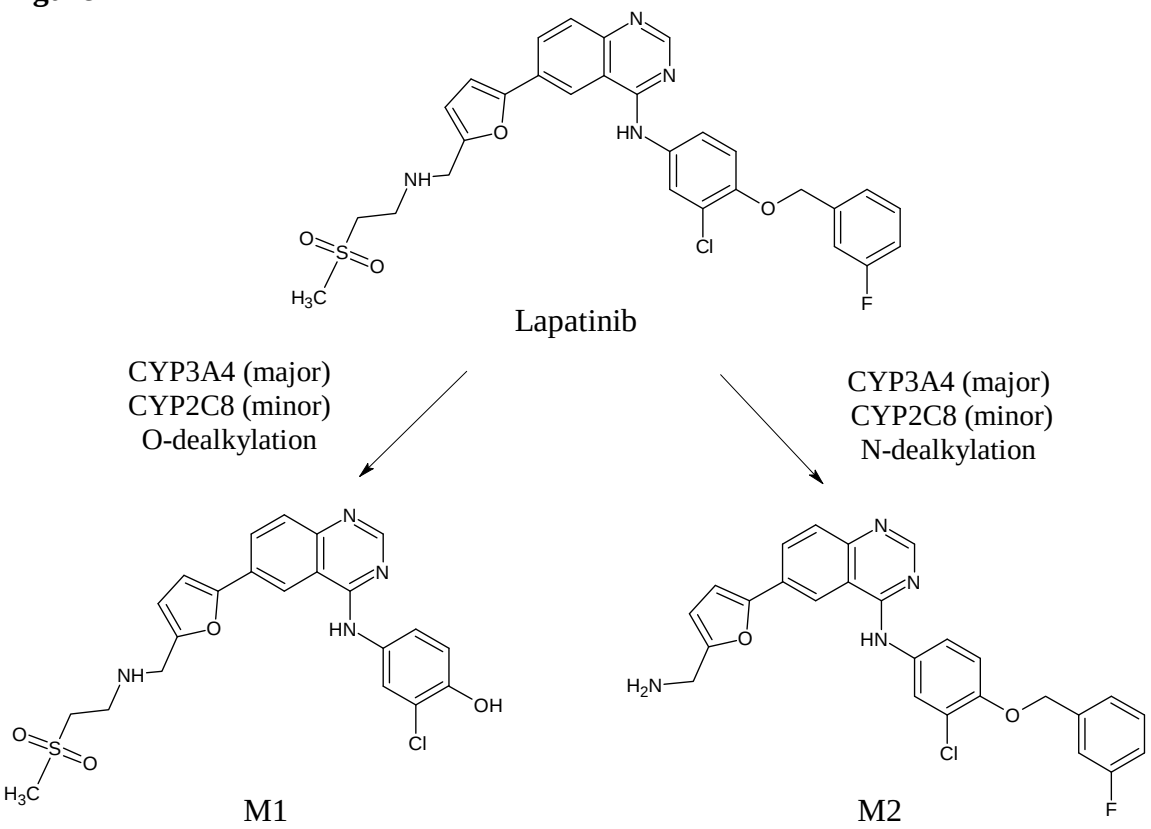

Molecular Pharmacology Fast Forward. Published on July 12, 2010 as DOI: 10.1124/mol.110.065839
This article has not been copyedited and formatted. The final version may differ from this version.

Figure 2

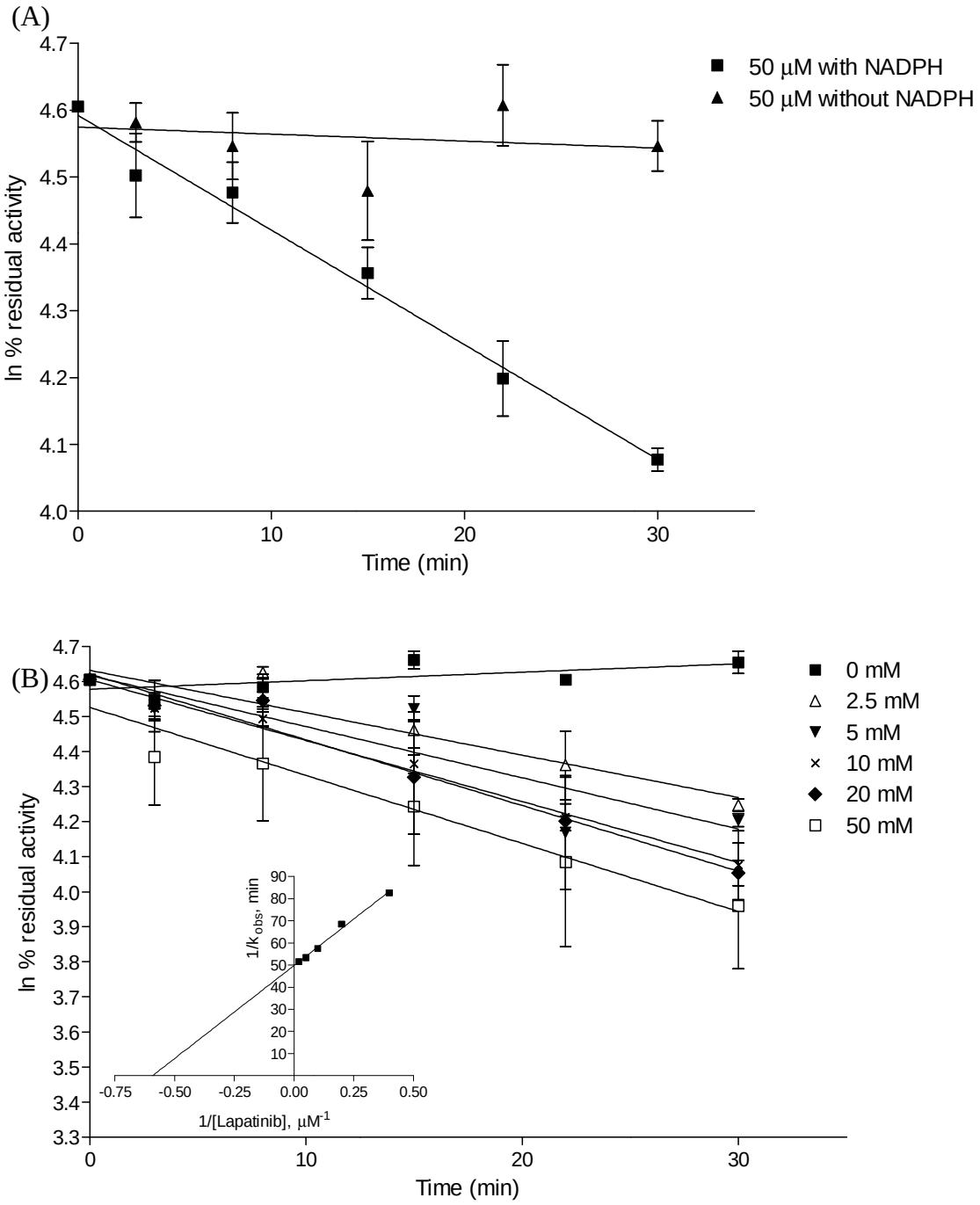

Figure 3

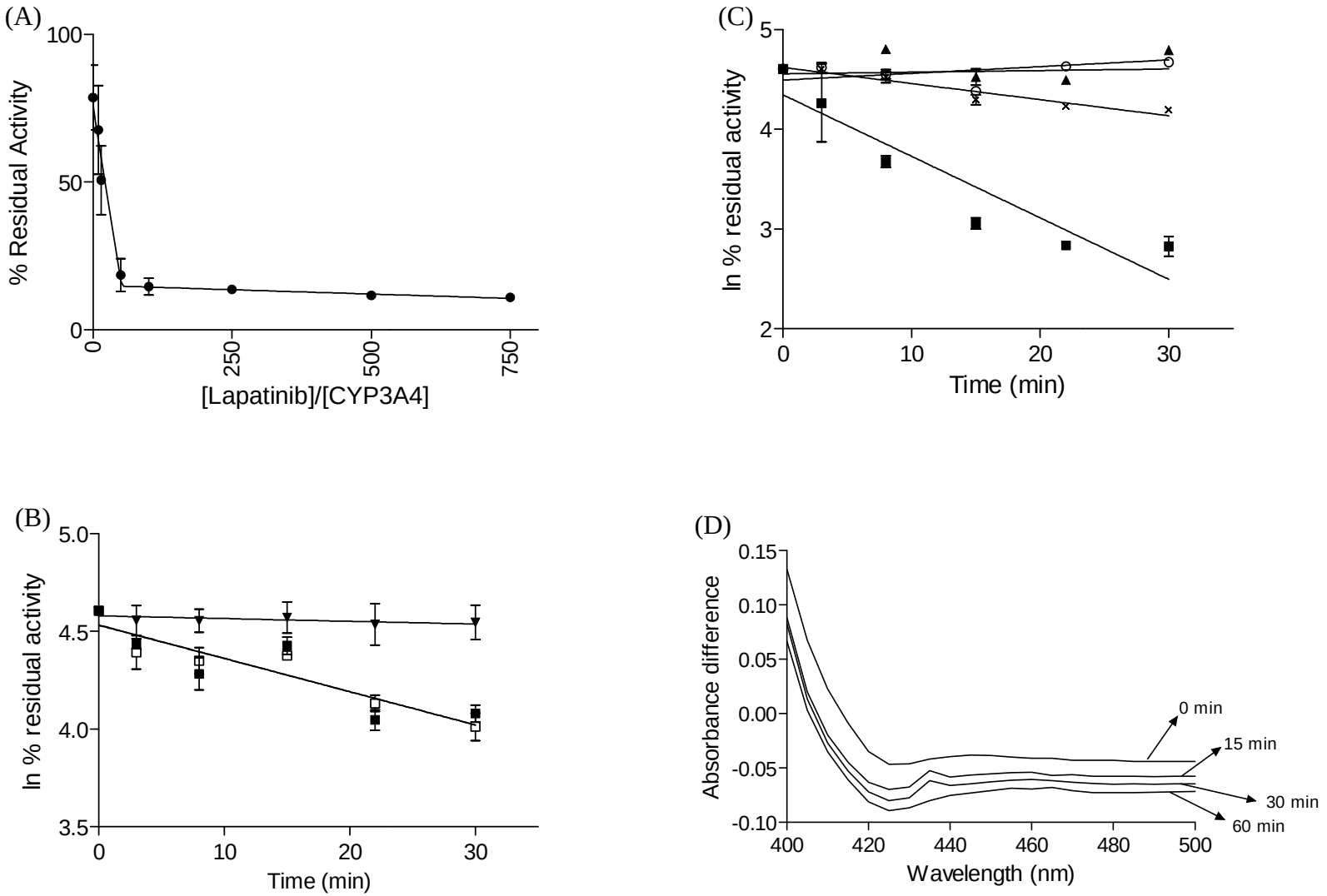

Molecular Pharmacology Fast Forward. Published on July 12, 2010 as DOI: 10.1124/mol.110.065839
This article has not been copyedited and formatted. The final version may differ from this version.

Figure 4

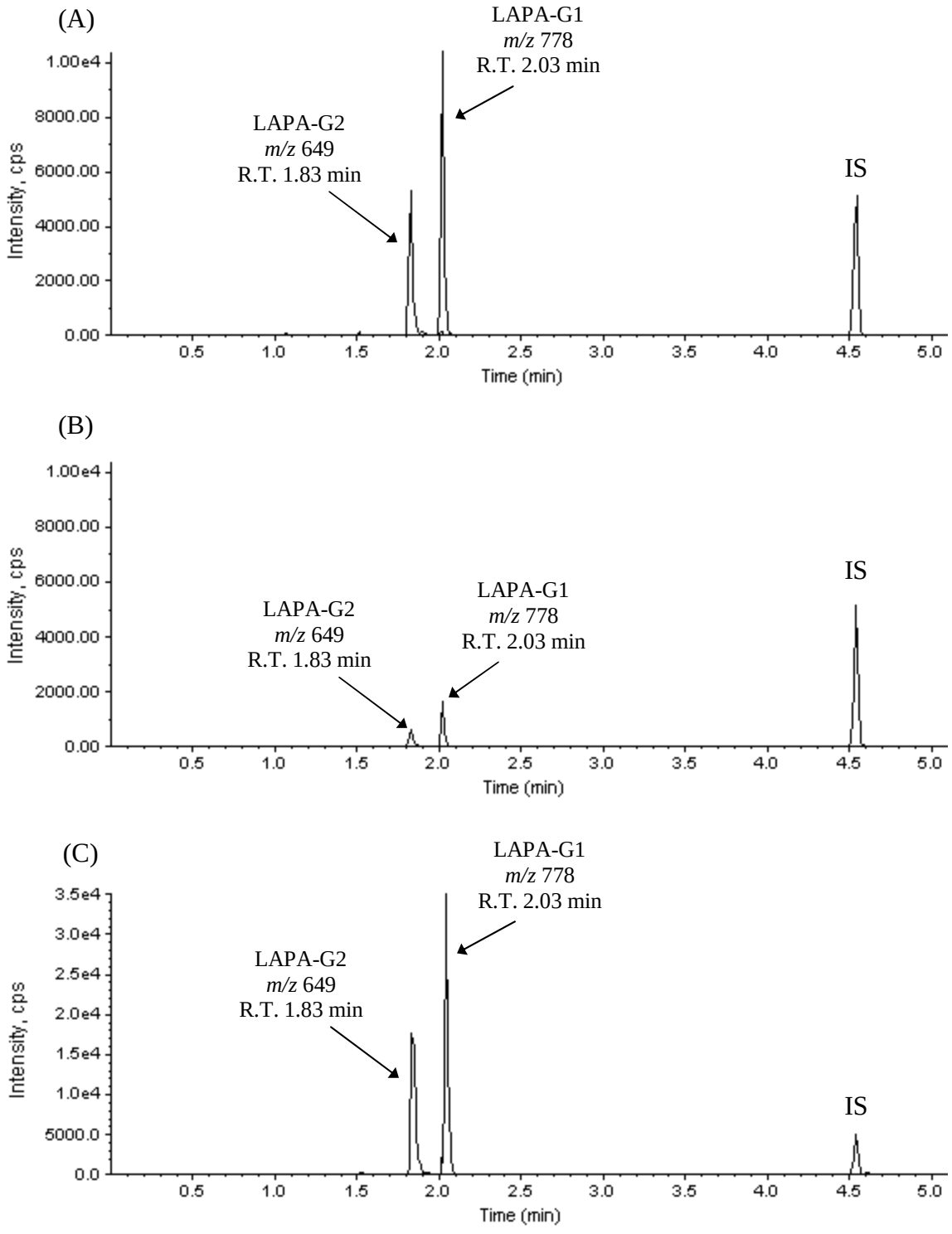

Molecular Pharmacology Fast Forward. Published on July 12, 2010 as DOI: 10.1124/mol.110.065839
This article has not been copyedited and formatted. The final version may differ from this version.

Figure 5

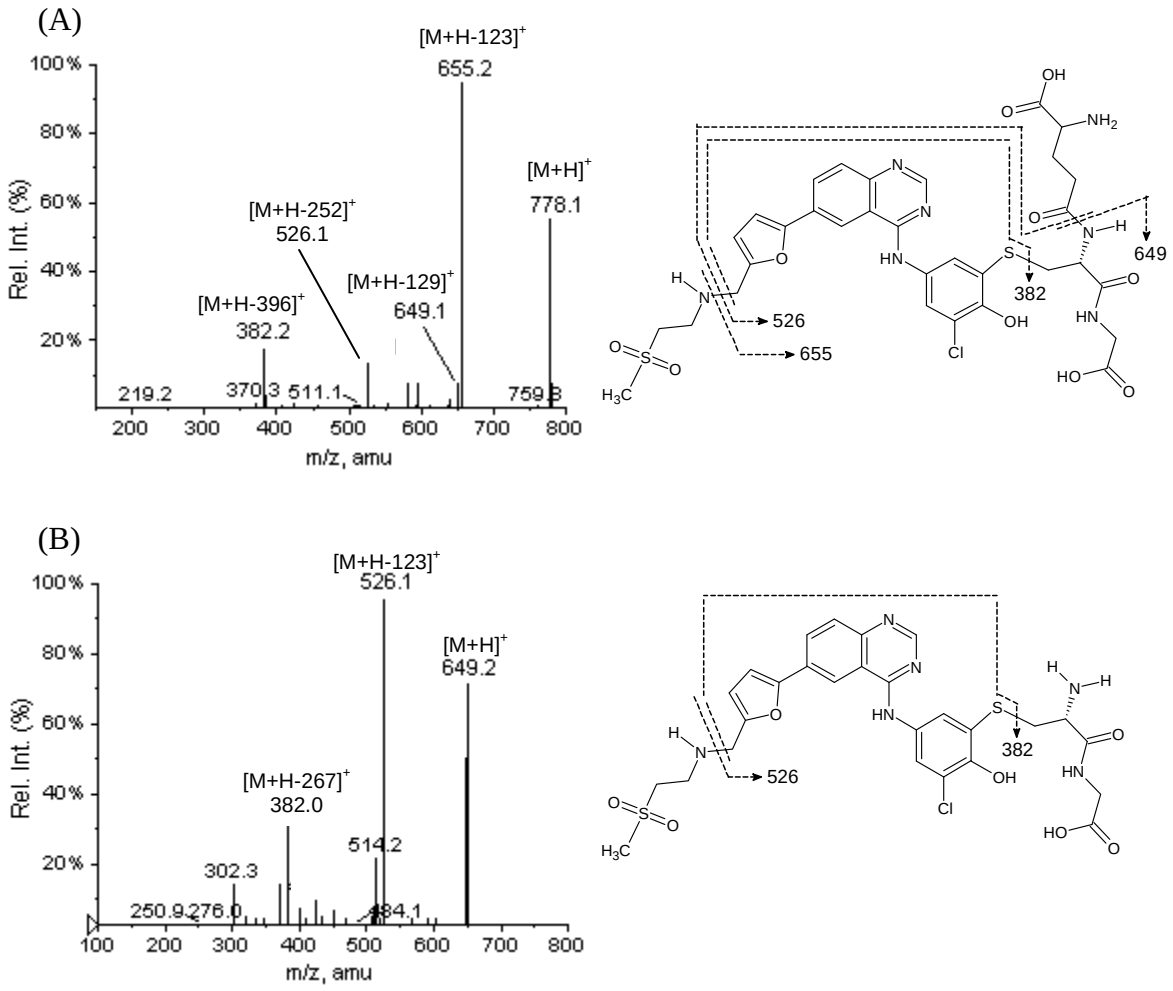

Figure 6